Journal of Magnetic Resonance 200 (2009) 313–320

Contents lists available at ScienceDirect

Journal of Magnetic Resonance

journal homepage: www.elsevier.com/locate/jmr

Comparison of NMR simulations of porous media derived from analytical and voxelized representations

Guodong Jin [a,1], Carlos Torres-Verdín [a,*], Emmanuel Toumelin [b]

[a] Department of Petroleum and Geosystems Engineering, The University of Texas at Austin, TX 78712, USA
[b] Chevron North America Exploration and Production, Houston, TX 77099, USA

ARTICLE INFO

Article history:
Received 12 May 2009
Revised 13 July 2009
Available online 22 July 2009

Keywords:
NMR response
Random-walk method
Grain pack
Voxel image
Surface-area effect

ABSTRACT

We develop and compare two formulations of the random-walk method, grain-based and voxel-based, to simulate the nuclear-magnetic-resonance (NMR) response of fluids contained in various models of porous media. The grain-based approach uses a spherical grain pack as input, where the solid surface is analytically defined without an approximation. In the voxel-based approach, the input is a computer-tomography or computer-generated image of reconstructed porous media. Implementation of the two approaches is largely the same, except for the representation of porous media. For comparison, both approaches are applied to various analytical and digitized models of porous media: isolated spherical pore, simple cubic packing of spheres, and random packings of monodisperse and polydisperse spheres. We find that spin magnetization decays much faster in the digitized models than in their analytical counterparts. The difference in decay rate relates to the overestimation of surface area due to the discretization of the sample; it cannot be eliminated even if the voxel size decreases. However, once considering the effect of surface-area increase in the simulation of surface relaxation, good quantitative agreement is found between the two approaches. Different grain or pore shapes entail different rates of increase of surface area, whereupon we emphasize that the value of the "surface-area-corrected" coefficient may not be universal. Using an example of X-ray-CT image of Fontainebleau rock sample, we show that voxel size has a significant effect on the calculated surface area and, therefore, on the numerically simulated magnetization response.

© 2009 Elsevier Inc. All rights reserved.

1. Introduction

Nuclear magnetic resonance (NMR) measurements have been used to study the structure of porous media and various processes occurring in them. They enable the estimation of many important petrophysical properties of porous media, including porosity, permeability, pore-size distribution, irreducible water saturation, oil viscosity, wettability, etc. Macroscopic descriptions of NMR measurements usually invoke the complicated diffusion-relaxation-dominated process in porous media [1].

Numerical simulations of NMR measurements in porous media are well established in literature. Different methods have been used to calculate NMR response, for example, the finite element method [2,3], the finite difference method [4], and the random-walk technique [1,5,7–18]. The finite difference and finite element approaches become computationally expensive for large and complicated three-dimensional (3D) porous structure [5,6], while the random-walk method is more often used to simulate the NMR response in the porous media because it is flexible and easy to implement and parallelize. Valfouskaya et al. [1] studied the time evolution of apparent diffusion coefficients in digitized models of various types of computer-generated porous media. Hidajat et al. [5] investigated the relationship between NMR response and permeability using synthetic models of porous media. Arns et al. [7] presented a comprehensive NMR response study of X-ray-CT (computed tomography) images obtained from rock samples. Øren et al. [8] compared the NMR response derived from reconstructed models, X-ray-CT images of Fontainebleau sandstone, and measurements. Ramakrishnan et al. [11] used ordered cubic packings of consolidated microporous spherical grains to study diffusion pore coupling phenomena in carbonate rocks. Toumelin et al. [12] generalized Ramakrishnan et al.'s model to include microscopic diffusion effects in the presence of a constant magnetic field gradient.

The above-described studies have dealt with either digitized models of porous media, in which the samples were approximately represented using an assembly of voxels [1,5,7–10], or models of spherical grain packs, where the geometries of porous media were analytically defined without approximation [11–14]. Modern NMR applications require simulation and interpretation methods that incorporate the complexity of real porous media at the pore scale.

* Corresponding author. Tel.: +1 512 471 4216; fax: +1 512 471 4900.
E-mail address: cverdin@mail.utexas.edu (C. Torres-Verdín).
[1] Present address: Baker Hughes Inc. 2001 Rankin Road, Houston, TX 77073, USA.

1090-7807/$ - see front matter © 2009 Elsevier Inc. All rights reserved.
doi:10.1016/j.jmr.2009.07.021

However, perhaps with the exception of sphere packs, it is generally impossible to characterize the detailed surface morphology of reservoir rocks. 3D images derived from high resolution X-ray computed tomography are only approximations of real porous media. It is unknown how these approximations of surface morphology affect the NMR response simulated with numerical methods.

Surface morphology of porous media plays a crucial role in magnetization relaxation processes. Due to the complex geometry of real porous material, it is difficult to quantify the impact of discretization of samples on simulation results. Peter et al. [19] found that discretization of actual phantom geometry yielded inaccurate simulations compared to those obtained with analytical phantoms in their Monte-Carlo simulations for nuclear biomedical application. Rajon et al. [20,21] emphasized that image voxelization overestimates the surface area of the bone-marrow interface, thereby leading to errors in cross-dose to bone as high as 25% for some low-energy beta emitters. They also found that the overestimation cannot be reduced through reduction of the voxel size (e.g., improved image resolution). NMR measurements, however, are very sensitive to pore-grain interfaces. It is not clear how numerically simulated NMR responses of porous media are influenced by sample discretization.

The objective of this paper is to analyze the effect of sample discretization on numerically simulated NMR responses. Clearly, to unravel the geometric information implicit in NMR relaxation measurements, one would like to perform the simulations in porous media with precisely known geometry. Sphere packs and their digitized representations provide an important benchmark system. We develop two different formulations of the random-walk technique to compute the time evolution of magnetization in porous media: one is based on spherical grain packs (*grain-based*), and the other is for digitized porous media (*voxel-based*). Both approaches follow exactly the same algorithm proposed in Refs. [22,23], except for the representation of porous media used in the model. In the grain-based model, we use a continuous smooth surface, whereas in the voxel-based model the surface is essentially truncated into a finite number of rectangular shapes.

The paper proceeds as follows: We first review the basic relaxation processes of spin magnetization in porous media and discuss different methods for treatment of local surface relaxation. In addition, we discuss the implementation of our random-walk simulation technique. Subsequently we describe the different models of porous media used to perform the numerical simulations. These models are analytically defined and discretized into their voxel counterparts. Finally, we present and compare results of simulations performed on these analytical and digitized models of porous media, with emphasis on the effect of discretization and voxel size. Salient conclusions are summarized in the last section.

2. Relaxation processes and random-walk simulation

2.1. Description of relaxation processes

For fluids in porous media, total magnetization originates from diffusion and relaxation processes and is sensitive to details of the microstructure of porous media. In this paper, we consider only transverse relaxation. Three independent processes are involved in describing the relaxation of spin magnetization [23]: (1) bulk fluid relaxation, with characteristic time T_{2B}, mainly due to dipole–dipole interactions between spins within the fluid; (2) surface relaxation, characterized by effective relaxation time T_{2S}, which is due to at least two effects: the additional interaction of protons at the pore-grain interface with paramagnetic impurities in the grains, and the hindered motion of water molecules in a layer adjacent to the pore-grain interface [24,25]; and (3) relaxation due to presence of background magnetic field heterogeneities, T_{2D}. Bulk and surface relaxation times are intrinsic properties governed by the fluid, the porous medium, and the thermodynamic state, while diffusion time is an experimentally controllable quantity affected by fluid diffusivity, internal fields induced by magnetic heterogeneities within the porous medium, and instrument configurations.

Surface morphology of porous media has a strong effect on the relaxation time T_{2S}, which in the fast-diffusion limit ($\rho R/D_B < 1$) is proportional to S/V [26], i.e.,

$$\frac{1}{T_{2S}} = \rho\frac{S}{V}, \tag{1}$$

where ρ is surface relaxivity, D_B is diffusion coefficient of bulk fluid, S is surface area of the pore, and V is pore volume. For a spherical pore of radius R, S/V is equal to $3/R$. Assuming no magnetic gradient in this study, the decay rate T_2 of the magnetization is given by

$$\frac{1}{T_2} = \frac{1}{T_{2B}} + \frac{1}{T_{2S}}. \tag{2}$$

2.2. Treatment of local surface relaxation

While spins remain away from a fluid boundary, the relaxation time T_2 is equal to the bulk fluid transversal relaxation times, T_{2B}. However, once spins are located within one step of a pore boundary of surface relaxivity ρ, the magnetization decay is locally enhanced to include the surface relaxation effect at the microscopic level. Most random-walk simulation models [1,5,7,13,15,16,18] assume that the spin has a probability p of being instantaneously "killed" (loosing completely its magnetization) when it reaches the boundary, and relate this probability to surface relaxivity ρ, for example, as [1,5,7,15]

$$p = A\frac{\rho\Delta r}{D_B} \times 0.96, \tag{3}$$

where Δr is the displacement the spin achieves during the interval $[t, t+\Delta t]$ when it reaches the boundary (also refer to Eq. (5)), and A is a correction factor of order 1 (usually set to 2/3) accounting for details of the random-walk implementation [15].

Alternatively, we use a more physical treatment of local surface relaxation [23]: The spin is not suddenly "killed", but instead its magnetization decreases by a factor $(1-p)$, or $\exp[\Delta t(p/\Delta t)]$ since $p \ll 1$. Therefore, the total relaxation rate becomes $1/T_2 = 1/T_{2B} + p/\Delta t$ for that step. Equivalently, the relaxation time used in each segment of the random walk becomes

$$\frac{1}{T_2} = \frac{1}{T_{2B}} + \chi\frac{3.84\rho}{\Delta r}, \tag{4}$$

where χ is the "surface-area-corrected" coefficient. In the grain-based model, $\chi = 1$ when the walker is located within a step of the relaxing boundary, and 0 otherwise. In the voxel-based model, the value of χ depends on the change of surface area due to discretizaton of a real surface. The constant 3.84 was obtained from $p/\Delta t$ using Eqs. (3) and (5).

2.3. Random-walk simulation method

Spin relaxation in the NMR response of a saturated porous system is simulated with the random-walk method, where we simulate the Brownian motion of a diffusing magnetized particle (walker). We have implemented two formulations for two different representations of porous media: spherical grain packs (*grain-based*) and digitized porous media (*voxel-based*). Both approaches

follow exactly the same algorithm proposed in Refs. [22,23], except for the representation of porous media used in the model.

In our model, starting points of walkers are randomly specified using a Monte Carlo algorithm. Only those walkers within the pore space occupied by fluids, i.e., water and/or oil, are retained. The walker distribution is proportional to the ratio of the volume of the oil phase to that of the water phase. Each walker is displaced for a sufficiently long time. When a walker attempts to step out of the pore space into the matrix, its magnetization decays with a rate determined by Eq. (4).

Length steps of a random walker depend on the type of porous media. At each time step of infinitesimal-duration, Δt, a vector of normally distributed random numbers $\vec{n} = (n_x, n_y, n_z)$ is generated with unit variance and zero mean. The walker is then spatially displaced in the Cartesian frame by a vector

$$\Delta\vec{r} = \sqrt{(6D_B\Delta t)}\,\frac{\vec{n}}{||\vec{n}||}. \tag{5}$$

In the grain-based approach, the time step is dynamically adapted along the walk so that (a) it is smaller than any magnetic-field pulse duration, (b) the amplitude of the total displacement, $\Delta\vec{r}$, is several times shorter than surrounding geometric length scales (e.g., pore throats restricting pore-to-pore connections, wetting film thickness, etc.), (c) the value of the total magnetic field can be assumed constant during each step, and (d) all walkers are synchronized at the onset and offset of magnetic pulses as well as at the time of echo acquisition [22,23].

However, for the voxel-based approach, we use two different fixed step sizes [27,28]: (1) if all 26 neighboring voxels of a pore voxel belong to the pore space of the same fluid phase, then the step size is equal to the voxel size, and (2) otherwise a small step size (several fractions of the voxel size) is used, which is determined by an input parameter. Two voxels (cubes) are considered to be neighbors if they have a common vertex, edge, or face. The time step is also dynamically adapted according to conditions (a)–(d) in the grain-based approach.

3. Models of porous media

In order to compare NMR responses obtained from analytical and digitized porous media, we first construct several "simple" models of porous media: the isolated spherical pore, simple cubic packing of spheres, and random packings of monodisperse and polydisperse spheres. The geometries of these models are analytically defined and subsequently discretized into voxel representations. Only random packings of monodisperse and polydisperse spheres are considered in this section. In addition, we simulate the NMR response of a high-resolution micro-X-ray-CT image of Fontainebleau sandstone.

The packing of monodisperse spheres is based on the real packing constructed by Finney [29], who measured the spatial coordinates of 8000 balls comprising the central part of the packing, in which 25000 mono-sized spherical ball bearings were packed densely. The size of ball bearings is 200 μm. Our simulation domain consists of 1000 spheres, whose spatial coordinates were obtained from Finney's data set and sphere diameter was increased to 220 μm (Fig. 1). Initial porosity is approximately 18.4%.

The random packing of polydisperse spheres is generated using the depositional model proposed in Refs. [30,31]. First, a number of spheres is generated according to a given probability distribution function. Then, the spheres are uniformly distributed within a domain without overlap. Thereafter, the spheres settle under gravity. Spheres can translate, rotate and rebound. The final equilibrium position of an individual sphere is determined by the balance of forces and moments acting upon it. Fig. 2 shows the computer-generated random sphere pack, which includes 2137 spheres with diameters uniformly distributed between 190 μm and 260 μm. The size of the non-uniform grain pack is 3000 μm × 3000 μm × 3458 μm, and its porosity is approximately 41.6%.

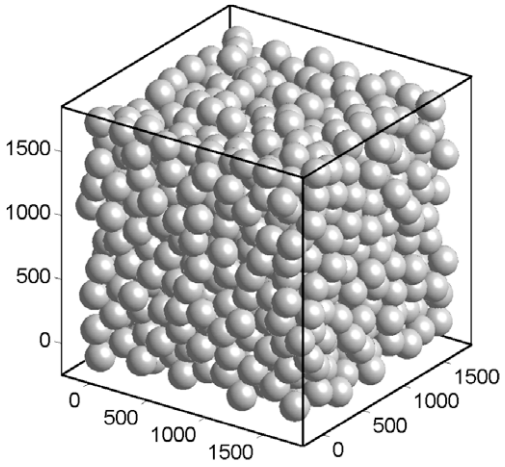

Fig. 1. Graphical description of the pack of 1000 monodisperse spheres. Dimensions of the pack are 2100 μm × 2100 μm × 2100 μm, with sphere diameter equal to 220 μm and porosity approximately equal to 18.4%.

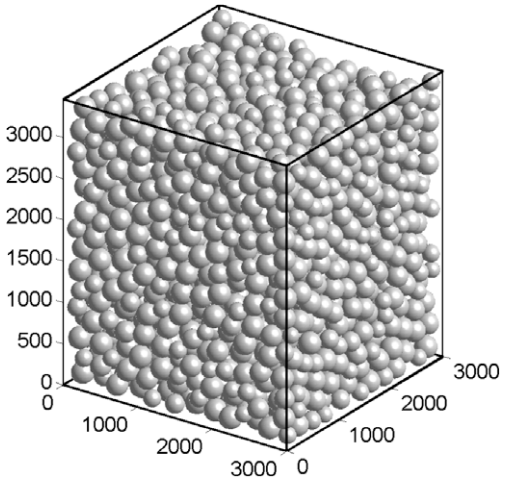

Fig. 2. Graphical illustration of the pack of 2137 polydisperse spheres. Dimensions of the packing are 3000 μm × 3000 μm × 3458 μm, with sphere diameters uniformly distributed between 190 μm and 260 μm. Porosity is approximately equal to 41.6%.

4. Results and analysis

In the following sections, we perform random-walk simulations to derive and compare NMR responses of the analytical and digitized porous media described above. We assume that porous media are fully brine-saturated in this study. Simulations were performed assuming a Carr–Purcell–Meiboom–Gill (CPMG) pulse sequence for transverse relaxation measurements with an inter-echo spacing of 1 *ms*. The T_{2B} value and the diffusion coefficient D_B for the bulk brine are chosen as 2800 *ms* and 2 μm²/ms, respectively. Relaxivity ρ is arbitrarily selected as 0.005 μm/*ms*. Simulations are stopped if the relaxation time is greater than 2000 *ms*. For comparison, the same values of these parameters are used in the simulations of grain- and voxel-based models.

4.1. Isolated spherical pore

For the single spherical pore of radius R shown in Fig. 3, the magnetization decay in the fast diffusion limit ($\rho R/D_B < 1$) is approximately given by the single exponential [5]

$$\frac{M(t)}{M_0} = \exp\left[-t\left(\frac{1}{T_{2B}} + \rho\frac{S}{V}\right)\right], \tag{6}$$

where M_0 is the initial transverse magnetization (equal to 1 in this study).

Fig. 4 compares the magnetization response $M(t)$ obtained from the grain-based simulation for the spherical pore of radius 8 μm (without discretization) to the analytical solution given by Eq. (6). These two methods give nearly identical results, thereby validating our grain-based random-walk simulation model. Note that Eq. (6) only gives an approximation of the exact solution. In the following, we assume that the result obtained from the grain-based simulation is the "exact" solution and hence is used as reference to compare results obtained with the voxel-based approach.

For simulations using the voxel-based approach, the isolated spherical pore and other samples in this study are discretized into a three-dimensional array of identical small cubes, referred to a *voxels*. We use the convention that a voxel is an element of the pore space if its center is in the pore space; otherwise, it is an element of the solid skeleton. Fig. 3 shows a schematic slice of the digitized spherical pore filled with yellow color. Fig. 5 shows the magnetization response numerically simulated with the voxel-based representation. Compared to the grain-based representation, the magnetization simulated with the voxel-based representation decays much faster. The difference in decay time is due to the discretization of the sample, given that both simulation approaches use the same algorithm and implementation method except for the representation of porous media (analytical and digitized models).

We use different voxel sizes to discretize the isolated spherical pore shown in Fig. 3. Fig. 6 describes the influence of voxel size on the time evolution of magnetization response $M(t)$. Clearly, the difference between simulations obtained with grain- and voxel-based approaches can be reduced (albeit not completely) if the voxel size is reduced, but what is not known is the minimum voxel size needed to reduce the difference to an acceptable value. Further, with smaller voxel sizes, constructing digital images (even a small piece) requires large computer resources for an increasing number of voxels. We conjecture that increasing the resolution (or reducing the voxel size) of a digitized image could not entirely eliminate the difference between the two simulation results due to the discretization of the sample.

Surface morphology of a digitized image is obviously different from its analytical counterpart. It is well known that the process of discretizing an analytically defined surface inevitably leads to errors because a continuous surface is truncated into a finite number of bins [19–21]. Table 1 describes results obtained from the discretization of a pore using different voxel sizes. One observes that the discretization of the pore space causes overestimation

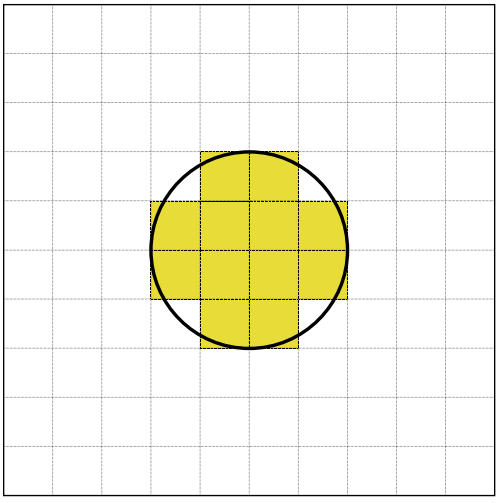

Fig. 3. Schematic diagram describing the discretization effect on the surface area of an isolated spherical pore. The solid circle indicates the true surface of the pore, while the yellow color denotes the corresponding pore in the digital image. (For interpretation of the references to color in this figure legend, the reader is referred to the web version of this paper.)

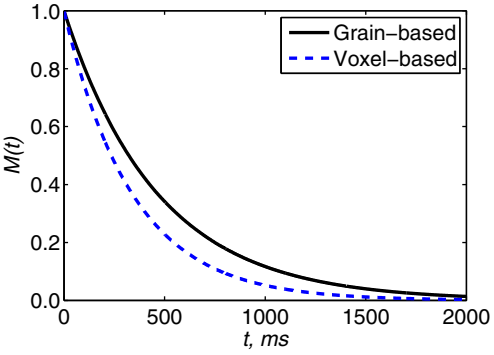

Fig. 5. Comparison of the magnetization response $M(t)$ for the isolated spherical pore obtained from grain- and voxel-based random-walk simulations. Voxel size is 1 μm.

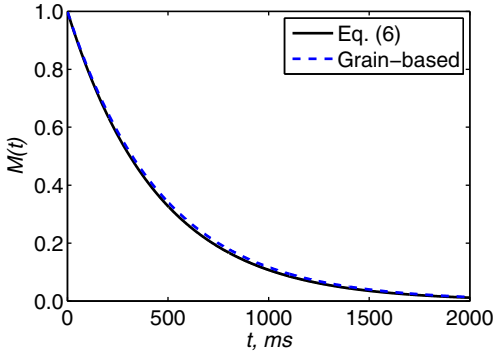

Fig. 4. Comparison of the magnetization response $M(t)$ for the isolated spherical pore obtained from grain-based random-walk simulations with Eq. (6). Simulations were performed with the assumption of $\rho R/D_B = 0.02$.

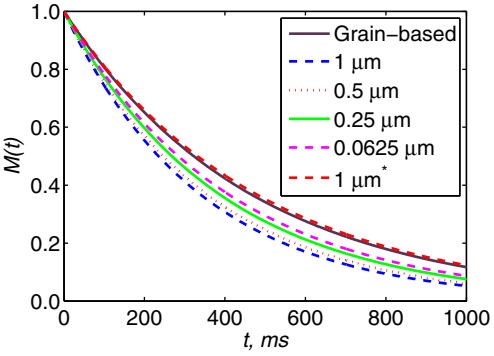

Fig. 6. Influence of voxel size on the magnetization response $M(t)$ for the isolated spherical pore derived from voxel-based simulations. The symbol "$*$" in the legend identifies simulation results obtained after considering increase of surface area.

(*about* 3/2) of the interface surface area which is not reduced with further reductions of voxel size. Intuitively, one can expect surface relaxation of spin magnetism to increase with increasing surface area (due to discretization) since it usually entails a higher probability for spins to make contact with the boundary in voxel-based images.

We emphasize that, for NMR simulations performed on the voxel-based images, the abnormal increase of surface area due to discretization should be taken into account when comparing results obtained with simulations based on analytical samples (without discretization). It becomes intuitive to set the "*surface-area-corrected*" coefficient χ in Eq. (4) to 2/3 (inverse of the increase of surface area) for simulations performed on digitized images, while χ remains 1 for analytical models. Fig. 6 shows simulation results obtained after considering the abnormal surface area increase. Results from both approaches are in very good agreement.

4.2. Simple cubic packing of spheres

To further investigate the effect of discretization on simulation results, we geometrically construct a simple cubic packing of mono-sized spheres. Dimensions of the packing are 200 μm × 200 μm × 200 μm, number of spheres is 125, and sphere radius is 20 μm. The sphere pack is discretized into voxel images using voxel sizes equal to 1 and 2 μm.

Fig. 7 shows simulation results obtained from grain- and voxel-based approaches. One observes that voxel size has null or marginal effect on simulation results when its value decreases below a certain value, for example 2 μm for this pack. In addition, discretization of the sample causes a significant difference in the magnetization response simulated with analytical and digitized models of the sphere pack. However, once we consider the effect of surface area increase, a good quantitative agreement is obtained between the two simulation approaches.

4.3. Random packing of monodisperse and polydisperse spheres

Models of porous media, such as the isolated spherical pore and simple cubic packing of mono-sized spheres, over-simplify the complex structure of porous media. In this section, we construct more complicated models of porous media: random packings of monodisperse and polydisperse spheres shown in Figs. 1 and 2, respectively. The packings are discretized into their voxel representations using voxel resolutions of 5 and 10 μm.

We simulate the NMR response of the fluid contained in the random sphere packs and their digital counterparts. Figs. 8 and 9 compare the simulated magnetization $M(t)$ obtained from grain- and voxel-based representations of the two packings. Results provide further evidence that the discretization leads to a significant difference in the simulated NMR response, while the effect of image resolution (voxel size) becomes negligible when the resolution

Table 1
Effect of voxel size on the pore volume and surface area of an isolated spherical pore of radius of 8 μm in the center of the cubic solid domain of size 20 μm × 20 μm × 20 μm shown in Fig. 3. The last rows describe the exact pore volume and surface area.

Voxel size (μm)	Voxels per dimension	Pore volume ($\times 10^3$ μm^3)	Surface area ($\times 10^4$ μm^2)
1	20	2.1760	0.1248
0.5	40	2.1570	0.1218
0.25	80	2.1465	0.1211
0.125	160	2.1468	0.1209
0.0625	320	2.1445	0.1206
–	–	2.1447	0.0804

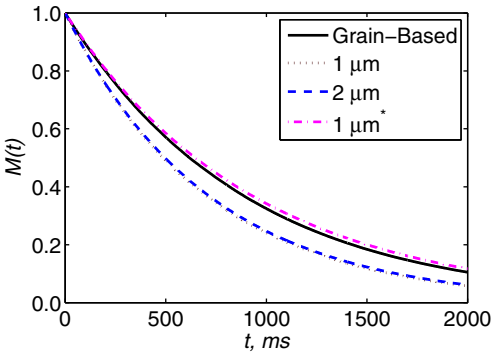

Fig. 7. Comparison of the magnetization response $M(t)$ obtained from grain- and voxel-based approaches for a simple cubic packing of mono-sized spheres. Sphere radius is 20 μm. The packing is discretized into voxel images using voxel sizes of 1 and 2 μm. The symbol "∗" in the legend identifies the simulation result obtained after considering the effect of increase of surface area.

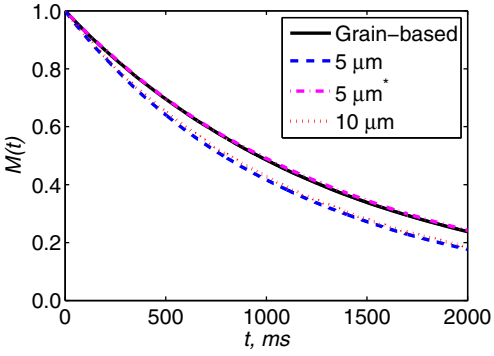

Fig. 8. Comparison of the magnetization response $M(t)$ obtained from grain- and voxel-based approaches for the random grain packing of mono-sized spheres shown in Fig. 1. Sphere diameter is 220 μm. The packing is discretized into voxel images using voxel sizes of 5 and 10 μm, respectively. The symbol "∗" in the legend identifies simulation results obtained after considering the effect of increase of surface area.

is large. It can be inferred that surface area, approximately 1.5 times greater than that of the continuum counterpart for the sphere pack, is not affected by voxel size when the latter is smaller than a certain critical value.

4.4. X-ray CT image

Simulations of the NMR response of sphere packs described in the preceding sections are valuable in that they provide an unambiguous analytical framework within which one can compare the effect of discretization on the magnetization response. However, the geometry of real porous materials is much more complicated and its details are very difficult to characterize. High resolution X-ray computed tomography is nowadays widely used to acquire three-dimensional images of porous materials. However, it is not clear how numerically simulated NMR responses are influenced by the digital approximation of the complex surface morphology of porous materials.

To further demonstrate the impact of discretization or voxel size on simulated NMR responses, we consider the micro X-ray-CT image shown in Fig. 10 of an actual Fontainbleau rock sample with porosity equal to 21.5%. Image size is 512 × 512 × 512 voxels, and voxel size is 5.68 μm. Porosity of the image is approximately 19.7%, slightly different from the measured rock porosity.

In order to construct images with different resolutions (voxel sizes), we decrease the resolution by replacing $n^3 (n = 2, 4, 8)$

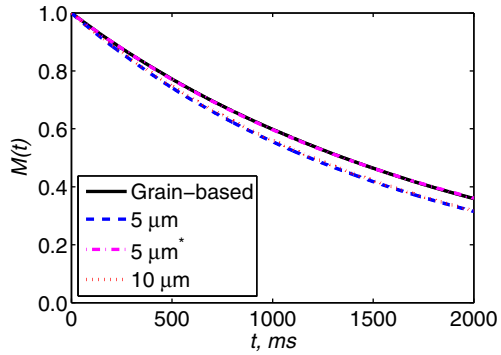

Fig. 9. Comparison of the magnetization response $M(t)$ simulated with grain- and voxel-based representations of the random grain packing of polydisperse spheres shown in Fig. 2. Sphere diameters are uniformly distributed between 190 μm and 260 μm, and the packing is discretized into images of voxel sizes of 5 and 10 μm. The symbol "$*$" in the legend identifies simulation results obtained after considering the effect of increase of surface area.

original neighboring voxels in the image with a coarser voxel. Each coarser voxel is assigned to an element of the pore space if more than 50% of its volume is within the pore space; otherwise, it becomes an element of the solid phase. In this manner, image resolution decreases and the geometry also changes. The original CT image of linear size equal to 512 voxels (denoted by C1) is changed to images of linear sizes equal to 256, 128, and 64 (denoted by C2, C4, C8, respectively).

Table 2 describes the influence of voxel size on image dimensions, porosity, and surface area. One observes that surface area increases with increasing image resolution (or decreasing voxel size). This change is also reflected on the simulated magnetization responses $M(t)$ shown in Fig. 11 for various images of different linear sizes. Results indicate that the decay rate of magnetization is enhanced as surface area increases. For reference purposes, we also show the experimental magnetization decay curve of a Fontainebleau sandstone sample with the same porosity of 21.5% [8], which may not be the sample used in our study. Note that relaxivity ρ and echo time in this simulation case are 0.015 μm/*ms* and 0.25 *ms*, respectively, which are the reported same values in Ref [8]. Bulk diffusion coefficient D_B and bulk relaxation time T_{2B} were not given

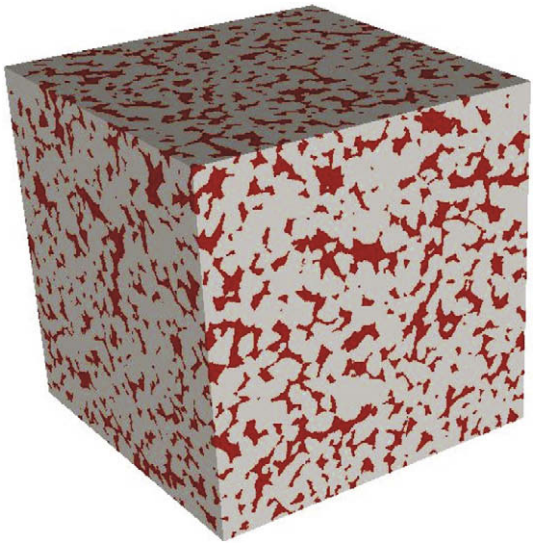

Fig. 10. Description of the $512 \times 512 \times 512$ X-ray-CT image. Gray and red colors denote the solid matrix and the pore space, respectively. Voxel size is 5.68 μm and porosity is approximately 19.7%.

Table 2
Effect of image resolution (voxel size) on image size, porosity, and surface area of the X-ray-CT image of Fontainebleau core sample shown in Fig. 10. Note that porosity and surface area are calculated directly from the image.

Image	Voxel size (μm)	Number of voxels per cartesian dimension	Porosity (%)	Surface area ($\times 10^8 \mu m^2$)
C1	5.68	512	19.7	5.28
C2	11.36	256	20.6	4.98
C4	22.72	128	18.9	4.06
C8	45.44	64	15.6	2.59

in Ref [8], and we arbitrarily set their values to 2.5 $\mu m^2/ms$ and 2800 *ms* [5], respectively.

The spatial resolution of 45.44 μm for image C8 is not sufficient to characterize the surface morphology of Fontainebleau sandstone, which is made up of well-sorted quartz grains with an average grain size of approximately 200 μm [8]. The simulated magnetization response for image C8 is apparently different from those obtained for images C1, C2 and C4. Results for images C1 and C2 are in good agreement. This observation indicates that a resolution of at least 11.36 μm may be needed to properly reproduce the 3D pore structure of such rock samples and to appraise the effect of discretization on the magnetization response of the digital image. In the simulation of surface relaxation, we set the "surface-area-corrected" coefficient χ in Eq. (4) to 2/3. This value was obtained from analysis of spherical grain packs. It is not clear how the surface area of a real rock sample will change after discretization.

4.5. Effect of pore shape on surface area

In the previous sections, we discussed in detail the effect of discretization or voxel size on simulated NMR responses. For spherical pores or spherical grain packs, it was found that discretization leads to an increase of surface area, approximately 1.5 times greater than that of the continuum counterpart. Different pore shapes have different specific surface areas; and the 1.5 multiple for increase may not be universal.

In order to quantify the effect of discretization on the surface area of pores with different shapes, we use alternative simple pore space geometries, such as ellipsoidal and cylindrical pores. Table 3 compares the surface area after discretization to that of analytical solutions for spherical, ellipsoidal, cylindrical, and cubic pores. Note that these pores are assumed aligned with the three Cartesian coordinate axes, that is, we ignore the effect of pore orientation. The pores have the same volume $\frac{4}{3}\pi \times 32\ \mu m^3$, and are discretized into their voxel representations using a resolution of 0.03125 μm. Except for the cubic pore, all pore shapes entail a certain amount of increase of surface area after discretization. One observes that the amount of increase is related to the specific surface area S_A/V. For ellipsoidal and cylindrical pores, the amount of increase becomes larger with decreasing specific surface area. However, such a conclusion cannot be generalized without a systematic investigation of different grain (or pore) shapes and orientations.

5. Discussion and conclusions

We introduced two different methods of random-walk simulation for diffusion-relaxation processes of fluids contained in porous media: grain- and voxel-based methods. Their implementation is exactly the same, except for the spatial representation of porous media. The grain-based model uses spherical grain packs as input, while the voxel-based one uses digital images of real or computer-generated samples. We tested and compared these two methods for several simple models of porous media: isolated spherical pore,

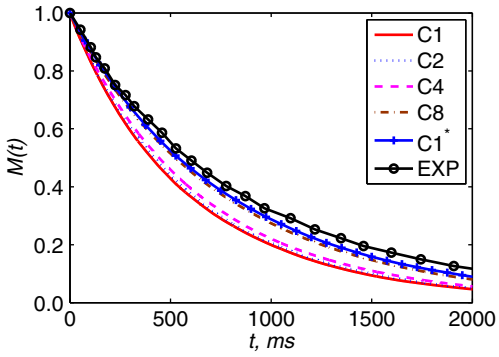

Fig. 11. Effect of image resolution (or voxel size) on the simulated magnetization response $M(t)$ for the X-ray-CT image of Fontainebleau rock sample shown in Fig. 10. The symbol "$*$" in the legend identifies simulation results obtained after considering the effect of increase of surface area, where the "surface-area-corrected" coefficient χ in Eq. (4) is set to 2/3. The curve denoted by EXP describes experimental data measured on a Fontainebleau sandstone sample (it may not be the sample used in this study) with porosity equal to 21.5% [8], and is included here only for reference purposes.

Table 3
Effect of discretization on the surface area of simple cubic, spherical, ellipsoidal, and cylindrical pores. The pores have the same pore volume $\frac{4}{3}\pi \times 32$ μm^3 and are aligned with Cartesian coordinate axes. Sphere radius is denoted by r_s, and the three principal semi-axes of the ellipsoid are denoted by a, b, and c. Cylinder radius and height are denoted by r_c and h, respectively. The side length of the cube is denoted by l. S_A is the exact surface area ($\times 10^2$ μm^2), S_A/V is the specific surface area of the pore (μm^{-1}), and S_D is the surface area after discretization ($\times 10^2$ μm^2).

Shape	Size	S_A/V	S_A	S_D	S_D/S_A
Sphere	$r_s = 3.175$	0.945	1.267	1.900	1.500
Ellipsoid	$a = 8, b = 4, c = 1$	1.646	2.206	2.765	1.253
Ellipsoid	$a = 8, b = 2, c = 2$	1.209	1.620	2.262	1.396
Ellipsoid	$a = 4, b = 4, c = 2$	1.035	1.388	2.011	1.450
Cylinder	$r_c = 8, h = 2/3$	3.250	4.356	4.441	1.020
Cylinder	$r_c = 4, h = 8/3$	1.250	1.676	1.855	1.107
Cylinder	$r_c = 8, h = 2/3$	1.188	1.592	1.957	1.229
Cube	$l = 5.118$	1.172	1.572	1.572	1.000

simple cubic packing of spheres, and random packings of monodisperse and polydisperse spheres.

Although only sphere packs can be used in the grain-based model, simulations obtained with such type of porous media are valuable in that they provide an unambiguous analytical framework wherein the NMR response can be simulated without discretization effects. This approach was validated by the agreement between the computed NMR response and the analytical solution for the case of an isolated spherical pore. The voxel-based method simulates the NMR response of fluids in more complex geometries (digitized representations) of porous media, which can be computer-tomography or computer-generated images. Because surface morphology of computer-generated porous media can change in a controlled manner, the voxel-based approach lends itself to a systematic study of diffusion and magnetic relaxation processes.

Surface morphology of porous media has a marked effect on magnetization relaxation processes. Compared to the grain-based method, in which the geometry of porous media is precisely and analytically defined, the voxel-based method uses a spacial approximation of continuous surfaces which results in an enhanced decay rate of spin magnetization. This enhanced decay rate is found to relate to the increase of surface area due to discretization of the sample. For sphere packs, discretization leads to an increase of surface area, approximately 1.5 times greater than that of the continuum counterpart. Overestimation of the surface area can not be eliminated with improved image resolution (reduction of voxel size). If the "artifact" increase of surface area is taken into account in simulations of surface relaxation, that is, the "surface-area-corrected" coefficient χ in Eq. (4) is set to 2/3 (inverse of the increase of surface area), a good quantitative agreement of the simulated magnetization response is found between grain- and voxel-based methods for sphere packs.

The effect of image resolution (voxel size) on simulated NMR responses was investigated on a X-ray-CT image of Fontainebleau sandstone. A 3D image is a digital representation of a real object. The interface between the solid and the pore space, which is most likely a curved surface in real porous materials, appears as a jagged surface in the 3D digital image due to the rectangular shape of the voxels. Consequently, a 3D digital image is not a realistic representation of the real sample. We found that the computed surface area of a digitized image increases with increasing resolution, hence resulting in an enhanced relaxation rate of spin magnetization. However, the surface area within the digitized image does not converge to the actual value even though the voxel size continues to decrease to an infinitely small value. It is not clear how much the surface area will change due to discretization since its 'exact' value is difficult to estimate from independent measurements. Therefore, it is unknown what value of "surface-area-corrected" coefficient χ in Eq. (4) should be used a priori in the simulation of surface relaxation.

Grain (or pore) shape has a substantial effect on the increase of surface area after discretization. Different shapes entail different rates of increase of surface area. It was found that the rate of increase is related to the specific surface area for ellipsoidal and cylindrical pores. The rate of increase grows with decreasing specific surface area, whereupon the value of the "surface-area-corrected" coefficient χ may not be universal. However, such a conclusion cannot be generalized without a systematic investigation of different grain (or pore) shapes and orientations. We conclude by noting that some of the preliminary observations presented in this paper can only be verified with a detailed study of a large number of pore-level simulations of digital images and laboratory measurements.

Acknowledgments

Our gratitude goes to the anonymous reviewer whose constructive, technical and editorial comments improved the paper.

The work reported in this paper was funded by the University of Texas at Austin's Research Consortium on Formation Evaluation, jointly sponsored by Anadarko, Aramco, Baker Hughes, BHP Billiton, BP, BG, ConocoPhillips, Chevron, ENI E&P, ExxonMobil, Halliburton Energy Services, Marathon Oil Corporation, Mexican Institute for Petroleum, Petrobras, Schlumberger, StatoilHydro, TOTAL, and Weatherford.

References

[1] A. Valfouskaya, P.M. Adler, J.-F. Thovert, M. Fleury, Nuclear magnetic resonance diffusion with surface relaxation in porous media, Journal of Colloid and Interface Science 295 (1) (2006) 188–201.
[2] S.H. Nguyen, D. Mardon, A p-version finite-element formulation for modeling magnetic resonance relaxation in porous media, Computers and Geosciences 21 (1) (1995) 51–60.
[3] H. Hagslätt, B. Jönsson, M. Nydén, O. Söderman, Predictions of pulsed field gradient NMR echo-decays for molecules diffusing in various restrictive geometries, Simulations of diffusion propagators based on a finite element method, Journal of Magnetic Resonance 161 (2) (2003) 138–147.
[4] G.Z. Zientara, J.H. Freed, Spin-echoes for diffusion in bounded, heterogeneous media: numerical study, J. Chem. Phys. 72 (1980) 1285–1292.
[5] I. Hidajat, M. Singh, J. Cooper, K.K. Mohanty, Permeability of porous media from simulated NMR response, Transport in Porous Media 48 (2) (2002) 225–247.
[6] K.K. Mohanty, J.M. Ottino, H.T. Davis, Reaction and transport in disordered composite media: introduction of percolation concept, Chemical Engineering Science 37 (1982) 905.

[7] C.H. Arns, A.P. Sheppard, R.M. Sok, M.A. Knackstedt, NMR petrophysical predictions on digitized core materials, Paper MMM, SPWLA 46th Annual Logging Symposium, New Orleans, Lousisiana, USA, 2005.
[8] P.E. Øren, F. Antonsen, H.G. Rueslåtten, S. Bakke, Numerical simulations of NMR responses for improved interpretations of NMR measurements in reservoir rocks, SPE 77398, SPE Annual Technical Conference and Exhibition, San Antonio, Texas, 2002.
[9] M. Regier, H.P. Schuchmann, Monte Carlo simulations of observation time-dependent self-diffusion in porous media models, Transport in Porous Media 59 (1) (2005) 115–126.
[10] S. Olayinka, M.A. Ioannidis, Time-dependent diffusion and surface-enhanced relaxation in stochastic replicas of porous rock, Transport in Porous Media 54 (3) (2004) 273–295.
[11] T.S. Ramakrishnan, L.M. Schwartz, E.J. Fordham, W.E. Kenyon, D.J. Wilkinson, Forward models for nuclear magnetic resonance in carbonate rocks, The Log Analyst 40 (4) (1999) 260–270.
[12] E. Toumelin, C. Torres-Verdín, S. Chen, Modeling of multiple echo-time NMR measurements for complex pore geometries and multiphase saturations, SPE Reservoir Evaluation & Engineering 6 (4) (2003) 234–243.
[13] L.M. Schwartz, J.R. Banavar, Transport properties of disordered continuum systems, Physical Review B 39 (16) (1989) 11965–11971.
[14] P.N. Sen, L.M. Schwartz, P.P. Mitra, B.I. Halperin, Surface relaxation and the long-time diffusion coefficient in porous media: periodic geometries, Physical Review B 49 (1) (1994) 215–225.
[15] D.J. Bergman, K.-J. Dunn, L.M. Schwartz, Self-diffusion in a periodic porous medium: a comparison of different approaches, Physical Review E 51 (4) (1995) 3393–3400.
[16] K.S. Mendelson, Percolation model of nuclear magnetic relaxation in porous media, Physical Review B 41 (1) (1990) 562–567.
[17] R.M.E. Valckenborg, H.P. Huinink, J.J.v.d. Sande, K. Kopinga, Random-walk simulations of NMR dephasing effects due to uniform magnetic-field gradients in a pore, Physical Review E 65 (2002) 021306.
[18] D.J. Wilkinson, D.L. Johnson, L.M. Schwartz, Nuclear magnetic relaxation in porous media: the role of the mean lifetime, Physical Review B 44 (10) (1991) 4960–4973.
[19] J. Peter, M.P. Tornai, R.J. Jaszczak, Analytical versus voxelized phantom representation for Monte Carlo simulation in radiological imaging, IEEE Transactions on Medical Imaging 19 (5) (2000) 556–564.
[20] D.A. Rajon, D.W. Jokisch, P.W. Patton, A.P. Shah, W.E. Bolch, Voxel size effects in three-dimensional nuclear magnetic resonance microscopy performed for trabecular bone dosimetry, Medical Physics 27 (11) (2000) 2624–2635.
[21] D.A. Rajon, P.W. Patton, A.P. Shah, C.J. Watchman, W.E. Bolch, Surface area overestimation within three-dimensional digital images and its consequence for skeletal dosimetry, Medical Physics 29 (5) (2002) 682–693.
[22] E. Toumelin, Pore-scale petrophysical models for the simulation and combined interpretation of nuclear magnetic resonance and wide-band electromagnetic measurements of saturated rocks, Ph.D. dissertation, The University of Texas at Austin, 2006.
[23] E. Toumelin, C. Torres-Verdín, B. Sun, K.-H. Dunn, Random-walk technique for simulating NMR measurements and 2D NMR maps of porous media with relaxing and permeable boundaries, Journal of Magnetic Resonance 188 (1) (2007) 83–96.
[24] J.R. Banavar, L.M. Schwartz, Probing porous media with nuclear magnetic resonance, Molecular Dynamics in Restricted Geometries, J. Klafter, J.M. Drake, Wiley, New York, 1989, 273–309.
[25] W.P. Halperin, F. D'orazio, S. Bhattacharja, J.C. Tarczon, Magnetic resonance relaxation analysis of porous media, Molecular Dynamics in Restricted Geometries, J. Klafter, J.M. Drake, Wiley, New York, 1989, pp. 311–350.
[26] K.R. Brownstein, C.E. Tarr, Importance of classical diffusion in NMR studies of water in biological cells, Physical Review A 19 (6) (1979) 2446–2453.
[27] G. Jin, C. Torres-Verdín, S. Devarajan, E. Toumelin, E.C. Thomas, Pore-scale analysis of the Waxman–Smits shaly-sand conductivity model, Petrophysics 48 (2) (2007) 104–120.
[28] G. Jin, C. Torres-Verdín, F. Radaelli, E. Rossi, Experimental validation of pore-level calculations of static and dynamic petrophysical properties of clastic rocks, SPE 109547, SPE Annual Technical Conference and Exhibition, Anaheim, California, November 11–14, 2007.
[29] J.L. Finney, Random packings and the structure of simple liquids. I. The geometry of random close packin, Proceedings of the Royal Society of London. Series A: Mathematical and Physical Sciences 319 (1539) (1970) 479–493.
[30] G. Jin, T.W. Patzek, D.B. Silin, Physics-based reconstruction of sedimentary rocks. SPE 83587, SPE Western Regional/AAPG Pacific Section Joint Meeting, Long Beach, California, May 19–24, 2003.
[31] G. Jin, Physics-based modeling of sedimentary rock formation and prediction of transport properties. Ph.D. dissertation, University of California at Berkeley, California, 2006.